

Noise-resilient penalty operators based on statistical differentiation schemes

Marc Vidal *^{1,2} and Yves Rosseel¹

¹DEPARTMENT OF DATA ANALYSIS, HENRI DUNANTLAAN 1, 9000 GHENT, BELGIUM

²MAX PLANCK INSTITUTE FOR HUMAN COGNITIVE AND BRAIN SCIENCES, LEIPZIG, GERMANY

marc.vidalbadia@ugent.be; yves.rosseel@ugent.be

Abstract

Penalized smoothing is a standard tool in regression analysis. Classical approaches often rely on basis or kernel expansions, which constrain the estimator to a fixed span and impose smoothness assumptions that may be restrictive for discretely observed data. We introduce a class of penalized estimators that operate directly on the data grid, denoising sampled trajectories under minimal smoothness assumptions by penalizing local roughness through statistically calibrated difference operators. Some distributional and asymptotic properties of sample-based contrast statistics associated with the resulting linear smoothers are established under Hellinger differentiability of the model, without requiring Fréchet differentiability in function space. Simulation results confirm that the proposed estimators perform competitively across both smooth and locally irregular settings.

AMS 2000 subject classifications: Primary 62G08; secondary 62G20.

Keywords: Asymptotic differentiability, Difference penalty, Discrete functional data, High-dimensional factor models, Semiparametric regression.

1. INTRODUCTION

Let (Ω, \mathcal{A}) be a measurable space, and let $\mathcal{M}_1(\mathbb{R}^d)$ denote the set of all probability measures on \mathbb{R}^d . We consider a parametric model $\mathcal{Q} = \{Q_\theta : \theta \in \Theta\}$ with open parameter domain $\Theta \subset \mathbb{R}^k$, where each Q_θ specifies the law of a random vector $X = (X_1, \dots, X_d) \in \mathbb{R}^d$. The entries of X are real-valued random variables indexed by $t \in \mathcal{I}_d = \{1, \dots, d\}$. This index may reflect an underlying structure, such as time, spatial location or both, or represent a labelled set of features organized according to some regularity criteria (e.g., decreasing rearrangements).

We observe independent and identically distributed realizations $X_1, \dots, X_n \sim Q_\theta$, where n denotes the sample size and the ambient dimension d is treated as fixed throughout. We begin by defining the penalized estimator associated with an arbitrary single realization $X_i = (X_{i1}, \dots, X_{id})$, and subsequently study its statistical properties when aggregated across the sample. Here, we interpret each X_i as a noisy discretization of a curve indexed by time, with stochastic variation governed by a low-rank plus noise structure represented by Q_θ . We therefore impose smoothness directly on discretized data using structured penalization, without invoking continuous function spaces or classical smoothness assumptions. To that extent, we define a penalized estimate \hat{X}_i as the solution to

$$\hat{X}_i(R; \alpha) = \arg \min_{f \in \mathbb{R}^d} \left\{ \frac{1}{2} \|X_i - f\|^2 + \sum_{r=1}^R \alpha_r \|D^{(r)} f\|^2 \right\}, \quad (1)$$

where $D^{(r)} \in \mathbb{R}^{d_r \times d}$ is a discrete difference operator of order r , and the weights $\alpha_r > 0$ control the strength of penalization at each derivative order. This formulation reflects a multiscale decomposition of variability, where each term $\|D^{(r)} f\|^2$ penalizes local roughness or curvature. In our implementation of (1), the operators $D^{(r)}$ are derived from finite difference stencils calibrated under a white noise model, ensuring that the penalties are unbiased in expectation.

Our penalized smoothing framework bears resemblance to kernel and spline regression (Müller, 1987; Hall and Opsomer, 2005), but differs in key respects. Rather than embedding the data into a predefined function space and estimating a smooth curve over a continuous domain, we consider the discrete data grid as the primary object of analysis (Mizuta, 2006, 2023), treating observations as high-dimensional vectors whose variation may exhibit low-rank structure or temporal dependence, as often encountered in factor models (Bai and Li, 2012). We impose roughness penalties based on discrete difference operators informed by a statistical noise model, aiming to attenuate incoherent variation without relying on pointwise evaluation or tuning the dimension of a basis expansion. While Hall and Opsomer (2005) analyze penalized spline estimators by embedding them into continuous white noise models to derive asymptotic properties, our approach

***Funding:** The authors acknowledge the support from the FWO project G013024N.

inverts this logic: we begin with discrete observations and formulate roughness penalties directly on the grid, statistically tailored to a white noise model, and derive theoretical guarantees without invoking continuous-function approximations. This perspective is motivated by recent work noting that preliminary smoothing, often treated as a benign preprocessing step, can implicitly impose regularity assumptions and affect the statistical interpretation of the data (Belhakem et al., 2025).

To place this grid-level refinement in an asymptotic setting, we appeal to the framework of asymptotic differentiability developed by Schick (2001). A central object of interest is the model-implied smoothed curve $f_\alpha(\vartheta)$, representing the expected output of the penalized smoother under the data-generating law Q_ϑ . In frameworks based on Fréchet differentiability, the map $\vartheta \mapsto f_\alpha(\vartheta)$ is assumed to be differentiable in a normed function space, so that small changes in ϑ translate directly into smooth changes in the regularized curve. In contrast, we rely on Hellinger differentiability of Q_ϑ , in the sense of Schick (2001), which guarantees that the square-root densities associated with the model vary smoothly in L^2 . This condition suffices to establish asymptotic properties of contrast-based statistics, without requiring the map $\vartheta \mapsto f_\alpha(\vartheta)$ to be differentiable in a functional sense. While our method assumes fixed and regular grids, it remains applicable to semi-dense sampling and may be extended to irregular or sparse designs using localized stencils or low-rank imputation.

2. DIFFERENCE OPERATORS WITH DECORRELATION PROPERTIES

A discrete difference operator of order r is a linear map $D^{(r)} : \mathbb{R}^d \rightarrow \mathbb{R}^{d_r}$, defined by a convolution with a fixed stencil of signed weights $w_{-L_r}^{(r)}, \dots, w_{L_r}^{(r)}$, where the stencil has symmetric support of length $2L_r + 1$ around the central index $\ell = 0$. The operator acts on a vector $x \in \mathbb{R}^d$ as

$$(D^{(r)}x)(t) = \sum_{\ell=-L_r}^{L_r} w_\ell^{(r)} x_{t+\ell},$$

for all $t \in \mathcal{J}^{(r)} = \{L_r + 1, \dots, d - L_r\}$, where the stencil is fully supported. The output dimension is $d_r = d - 2L_r$. Common difference operators fix weights $w_\ell^{(r)}$ using binomial coefficients from Pascal's triangle, which can be aligned to produce forward, backward, or centred differences. In contrast, our weights are constructed to satisfy statistical rather than purely algebraic properties. While the framework allows for general (possibly asymmetric) stencils, we focus on symmetric constructions, those satisfying $w_\ell^{(r)} = (-1)^\ell w_{-\ell}^{(r)}$, which arise naturally in our approach.

Following Mizuta (2023), we consider a white noise model $Q_0 \in \mathcal{M}_1(\mathbb{R}^d)$ under which the entries of $X = (X_1, \dots, X_d)$ are independent standard normal random variables. Accordingly, $E_{Q_0}(X) = 0$ and $\text{cov}_{Q_0}(X) = I_d$, so for any fixed linear operator $D^{(r)}$, the transformed vector $D^{(r)}X$ has zero mean and variance structure determined entirely by the stencil weights. In particular, classical difference operators generally yield correlated outputs when applied to white noise. To prevent such operators from introducing spurious structure, we construct a family of *uncorrelated difference operators* $\bar{D}^{(r)}$ recursively so that

$$\text{cov}_{Q_0} \{(\bar{D}^{(r)}X)_t, (\bar{D}^{(s)}X)_t\} = 0 \quad \text{for all } s < r \text{ and all } t, \quad \text{and} \quad \text{var}_{Q_0} \{(\bar{D}^{(r)}X)_t\} = 1.$$

We now verify that the explicit stencil constructions satisfy the required decorrelation conditions under the white noise model Q_0 . Although Mizuta (2023) provides concrete weights for the first few operators, no general closed-form expression or recursive derivation scheme is given. The first four uncorrelated difference operators $\bar{D}^{(r)}$ are listed below, all expressed as a finite stencil centered at t_j . Each row gives the (unnormalized) stencil weights applied to a grid window centered at location t_j , spanning positions $t_{j+\ell}$ for $\ell = -5, \dots, 5$, as displayed in the stencil layout.

	t_{j-5}	t_{j-4}	t_{j-3}	t_{j-2}	t_{j-1}	t_j	t_{j+1}	t_{j+2}	t_{j+3}	t_{j+4}	t_{j+5}
$\bar{D}^{(0)}$	0	0	0	0	0	1	0	0	0	0	0
$\bar{D}^{(1)}$	0	0	0	0	1	0	-1	0	0	0	0
$\bar{D}^{(2)}$	0	0	0	1	-1	0	-1	1	0	0	0
$\bar{D}^{(3)}$	0	0	2	-3	0	0	0	3	-2	0	0
$\bar{D}^{(4)}$	7	-16	9	0	0	0	0	0	9	-16	7

We now formalize the construction. Each operator $\bar{D}^{(r)}$ is defined as the solution to a constrained linear system enforcing (i) orthogonality to all lower-order stencils, (ii) zero mean, (iii) (anti)symmetry depending on parity of r , and (iv) unit

variance under Q_0 . If the solution is unique up to a scaling constant, we interpret $\bar{D}^{(r)}$ as a canonical representative of order- r roughness under the white noise model. In this case, the collection $\bar{D}^{(r)}$ forms an orthogonal basis for structured deviations from independence.

Proposition 2.1. *Let $L \in \mathbb{N}$, and let $\bar{D}^{(0)}, \dots, \bar{D}^{(r-1)} \in \mathbb{R}^{2L+1}$ be previously constructed, normalized stencil vectors following Mizuta's scheme. Each vector is indexed symmetrically by offsets $\ell = -L, \dots, L$, and centred at $\ell = 0$. Then the r th order uncorrelated difference operator $\bar{D}^{(r)} \in \mathbb{R}^{2L+1}$ is any unit-norm vector $w = (w_{-L}, \dots, w_0, \dots, w_L)$ satisfying:*

1. $w \perp \bar{D}^{(0)}, \dots, \bar{D}^{(r-1)}$,
2. $\sum_{\ell=-L}^L w_\ell = 0$,
3. $w_\ell = (-1)^\ell w_{-\ell}$ for all $\ell = -L, \dots, L$,
4. $\|w\| = 1$.

Let $\mathcal{V}_r \subset \mathbb{R}^{2L+1}$ denote the subspace defined by conditions (1)–(3). Then $\bar{D}^{(r)}$ is uniquely determined up to sign if and only if $\dim(\mathcal{V}_r) = 1$. In particular, for $L = 6$ (i.e., stencil length 13), the operators $\bar{D}^{(0)}, \dots, \bar{D}^{(4)}$ are uniquely defined under these constraints, while for $r = 5$, the solution is no longer unique.

Corollary 2.2. *Let $X \sim Q_0$, and let $\bar{D}^{(0)}, \dots, \bar{D}^{(R)} \in \mathbb{R}^{2L+1}$ be the stencil vectors from Proposition 2.1, constructed using a common half-width L , with $R \leq 4$. For each r , define $Y^{(r)} = \bar{D}^{(r)} X \in \mathbb{R}^{d-2L}$. Then, for all valid t :*

1. $E_{Q_0}(Y^{(r)}) = 0$ and $\text{var}_{Q_0}(Y_t^{(r)}) = 1$;
2. $\text{cov}_{Q_0}(Y_t^{(r)}, Y_t^{(s)}) = 0$ for all $s < r$;
3. If $X \sim \mathcal{N}(0, I_d)$, then $Y_t^{(r)}$ and $Y_t^{(s)}$ are independent for $r \neq s$.

The uncorrelated operators $\bar{D}^{(r)}$ provide a scale-wise decomposition of discrete roughness under the white noise model Q_0 , analogous to Parseval's identity. A formal statement (Corollary A.1) and proof are provided in the [Appendix A](#).

3. DISCRETE SMOOTHING OPERATORS

3.1. Discrete penalization with finite differences

We begin by motivating our discrete penalty constructions from a continuous smoothing perspective. A common approach is to penalize the roughness by replacing the L^2 inner product with a Sobolev version of the form $\langle f, g \rangle_\alpha = \langle f, g \rangle_{L^2} + \alpha \langle f^{(r)}, g^{(r)} \rangle_{L^2}$, which induces the smoothing operator $S_\alpha^{(r)} = (\mathbb{I} + \alpha \mathcal{D}^{(r)*} \mathcal{D}^{(r)})^{-1}$, where $\mathcal{D}^{(r)}$ denotes the r th derivative operator, $\mathcal{D}^{(r)*}$ its adjoint, and \mathbb{I} represents the identity in the space. This operator serves as the continuous prototype for our discrete penalty framework.

To mirror the role of the continuous derivative $f^{(r)}$, we represent its discrete analogue as a matrix $D^{(r)} \in \mathbb{R}^{d' \times d}$, which acts linearly on data vectors in \mathbb{R}^d . Given a observed trajectory $X_i \in \mathbb{R}^d$, we define the roughness penalty $X_i^\top \mathfrak{P} X_i = \|D^{(r)} X_i\|^2$, where $\mathfrak{P} = (D^{(r)})^\top D^{(r)}$, which acts as a discrete analogue of the Sobolev norm contribution. The associated discrete smoothing operator

$$S_\alpha^{(r)} = (I_d + \alpha \mathfrak{P})^{-1}, \tag{2}$$

yields the penalized estimator $\hat{X}_i = S_\alpha^{(r)} X_i$, corresponding to the solution of (1) for a single r .

At this level, the operator $D^{(r)}$ is kept generic and need not possess any specific statistical optimality properties. In particular, classical finite-difference operators generally induce correlated outputs when applied to noise. To ensure that the penalty reflects genuine structural deviations rather than artefacts of the differencing scheme, we construct \mathfrak{P} with respect to a reference noise model, typically a white noise law Q_0 . In this case, $D^{(r)}$ is replaced by a statistically calibrated operator $\bar{D}^{(r)}$. The resulting penalty matrix then encodes distributional constraints on roughness, ensuring sensitivity to departures from pure noise while avoiding spurious correlations. Under this perspective, the model Q_θ can be viewed as the convolution of a distribution encoding structural dependence (e.g., smoothness) with a noise distribution, and the discrete smoothing operator (2) acts to attenuate noise while preserving statistically relevant directions.

In the following subsections, we describe two extensions: single-step convex penalization and sequential multi-resolution smoothing.

3.2. Smoothing with convex roughness penalties (fixed order)

When the observational noise exhibits temporal dependence (e.g., coloured or autocorrelated noise), strict reliance on either standard or uncorrelated penalties may be suboptimal. Standard difference penalties implicitly allow correlations across derivative levels, while uncorrelated differences enforce statistical separation tailored to white noise. In intermediate regimes, convex combinations provide a flexible compromise, allowing the smoother to adapt to the underlying noise structure.

We therefore define a class of penalty operators that interpolate between standard and uncorrelated difference penalties. Let \mathfrak{P} and \mathfrak{P}_{Q_0} denote the penalty matrices associated with conventional and uncorrelated discrete differences of fixed order r , respectively. We form the convex combination

$$\mathfrak{P}_\eta = (1 - \eta) \mathfrak{P} + \eta \mathfrak{P}_{Q_0}, \quad \eta \in [0, 1],$$

where η controls the relative contribution of each component. The resulting smoothing operator is $S_{\alpha, \eta}^{(r)} = (I_d + \alpha_r \mathfrak{P}_\eta)^{-1}$, which interpolates between standard penalization ($\eta = 0$) and purely uncorrelated penalization ($\eta = 1$). Since both \mathfrak{P} and \mathfrak{P}_{Q_0} are symmetric and positive semi-definite, their convex combination inherits these properties, ensuring well-posedness of the penalized estimator. In practice, a simple autocorrelation analysis of the observed curves can guide the choice of η , with stronger dependence favouring standard penalties and weaker dependence favouring uncorrelated ones.

3.3. Sequential and simultaneous multi-resolution smoothing

We consider two complementary strategies for penalized smoothing across multiple derivative orders. Both strategies can be implemented either with purely uncorrelated penalties \mathfrak{P}_{Q_0} or with interpolated penalties \mathfrak{P}_η at each order.

Sequential (adaptive) smoothing. In the sequential approach, smoothing is applied iteratively across decreasing derivative orders, starting from the highest order R and proceeding down to first order. At each step r , we solve

$$f_r = \arg \min_{f \in \mathbb{R}^d} \left\{ \frac{1}{2} \|f - f_{r+1}\|^2 + \alpha_r f^\top \mathfrak{P}_\eta f \right\}, \quad (3)$$

where f_{r+1} denotes the estimate from the previous step, with initialization $f_{R+1} = X_i$. The solution is explicit and given by $f_r = (I_d + \alpha_r \mathfrak{P}_\eta)^{-1} f_{r+1}$. This formulation allows order-specific regularization while adapting locally to structure present at each resolution level.

Simultaneous (multi-order) smoothing. In contrast, the simultaneous strategy applies a single update using an aggregate penalty that combines contributions across all derivative orders:

$$\mathfrak{P}_\eta^{(1:R)} = \sum_{r=1}^R \alpha_r \left\{ (1 - \eta) D^{(r)\top} D^{(r)} + \eta \bar{D}^{(r)\top} \bar{D}^{(r)} \right\}.$$

The resulting estimator is $\hat{X}_i = (I_d + \mathfrak{P}_\eta^{(1:R)})^{-1} X_i$, yielding a one-step solution that balances smoothness across scales through fixed weights.

Both approaches reduce to standard multi-order penalization when $\eta = 0$, and to multi-order uncorrelated penalization when $\eta = 1$.

4. LOCAL STABILITY AND ASYMPTOTIC LINEARITY UNDER HELLINGER DIFFERENTIABILITY

We consider a finite-dimensional parametric model $\mathcal{Q} = \{Q_\vartheta : \vartheta \in \Theta \subset \mathbb{R}^k\}$, where each $Q_\vartheta \in \mathcal{M}_1(\mathbb{R}^d)$ is a distribution over discretized curves $X \in \mathbb{R}^d$. Assume that each Q_ϑ admits a density f_ϑ with respect to a common dominating measure μ , and define $s_\vartheta = f_\vartheta^{1/2} \in L^2(\mu)$. We say that the model \mathcal{Q} is *Hellinger differentiable* at a point $\tau \in \Theta$ if the square-root densities s_ϑ vary smoothly in $L^2(\mu)$ around τ (Schick, 2001). Formally, this means there exists a function $\kappa_\tau : \mathbb{R}^d \rightarrow \mathbb{R}^k$, called the *Hellinger score*, satisfying

$$\int \kappa_\tau \, dQ_\tau = 0, \quad \int \|\kappa_\tau\|^2 \, dQ_\tau < \infty,$$

such that the approximation

$$\int \left(s_\vartheta - s_\tau - \frac{1}{2} (\vartheta - \tau)^\top \kappa_\tau s_\tau \right)^2 \, d\mu = o(\|\vartheta - \tau\|^2),$$

holds as $\vartheta \rightarrow \tau$. This condition implies that $s_\vartheta \in L^2(\mu)$ is Fréchet differentiable at τ , with derivative $\partial_\vartheta s_\vartheta|_{\vartheta=\tau} = \frac{1}{2} \kappa_\tau \cdot s_\tau$.

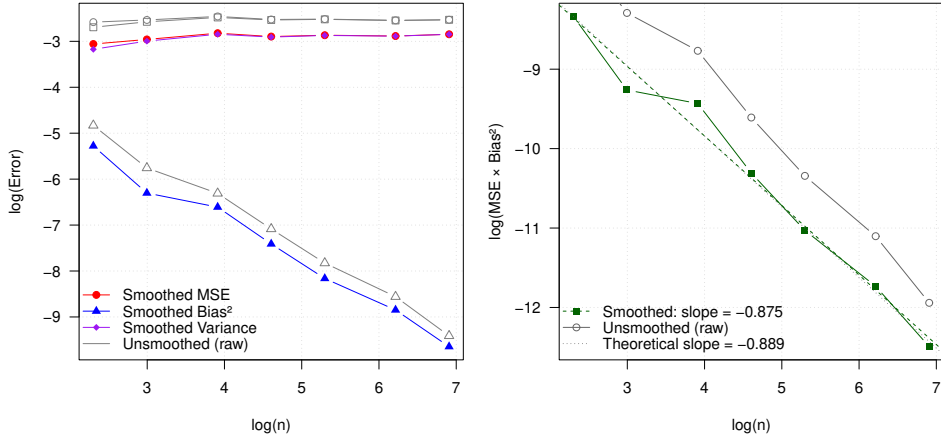


Figure 1: Empirical convergence of discrete penalized smoothing. *Left:* Log–log plots of the mean squared error (MSE), squared bias, and variance of the sample-averaged smoothed estimator ($r = 2, \eta = 0.5$) as functions of the sample size n , with unsmoothed (raw) counterparts shown in grey for comparison. *Right:* Log–log plot of $\text{MSE} \times \text{Bias}^2$, illustrating the bias–variance trade-off and the associated decay behaviour.

Assuming that the model \mathcal{Q} is Hellinger differentiable, we can proceed with the construction of contrast-based inference procedures. Consider the model-implied smoothed mean

$$f_\alpha(\vartheta) = E_{Q_\vartheta}(S_\alpha X) = S_\alpha m_\vartheta,$$

which serves as the population centring of the smoothed contrast. Henceforth, let S_α denote a fixed, linear and bounded discrete smoothing operator, and assume that X_1, \dots, X_n are i.i.d. \mathbb{R}^d -valued random vectors with common law Q_ϑ .

For fixed α , define the centred contrast

$$h_\vartheta^{(\alpha)}(X_i) = S_\alpha X_i - f_\alpha(\vartheta), \quad (4)$$

which satisfies $E_{Q_\vartheta}\{h_\vartheta^{(\alpha)}(X)\} = 0$. To ensure sensitivity of the contrast to perturbations of ϑ , we impose the following regularity conditions: (i) the family of covariance matrices $\Sigma_\vartheta \in \mathbb{R}^{d \times d}$ is uniformly non-singular, i.e., $\sigma_{\min}(\Sigma_\vartheta) \geq c > 0$ for all $\vartheta \in \Theta$; (ii) the smoothing operator S_α is fixed, linear and uniformly bounded in operator norm.

Under these conditions, the map $\vartheta \mapsto s_\vartheta \in L^2(\mu)$ is Fréchet differentiable, and since S_α is a fixed bounded operator, the smoothed target $f_\alpha(\vartheta) = E_{Q_\vartheta}(S_\alpha X)$ inherits this regularity. Henceforth we assume that X_1, \dots, X_n are i.i.d. \mathbb{R}^d -valued random vectors with common law Q_ϑ . For a fixed α , recall the centred contrast (4). Then, to ensure asymptotic linearity of the contrast statistic

$$H_n^{(\alpha)}(\vartheta) = \frac{1}{\sqrt{n}} \sum_{i=1}^n h_\vartheta^{(\alpha)}(X_i), \quad (5)$$

we impose the following local stability condition.

Assumption 4.1. *There exists a bounded linear operator $\mathcal{L}_\tau : \mathbb{R}^k \rightarrow \mathbb{R}^d$ such that for every bounded sequence $g_n \in \mathbb{R}^k$,*

$$H_n^{(\alpha)}(\tau + n^{-1/2} g_n) - H_n^{(\alpha)}(\tau) - \mathcal{L}_\tau g_n \xrightarrow{P_\tau} 0 \quad \text{as } n \rightarrow \infty.$$

This assumption ensures a locally linear expansion of the contrast statistic (5) under root- n perturbations of ϑ . Theorem 2.3 of Schick (2001) requires the model to be Hellinger differentiable and that the map $\vartheta \mapsto h_\vartheta^{(\alpha)} \in L^2(Q_\vartheta)$ to be Hellinger continuous. According to his Lemma 2.5, this continuity is equivalent to two conditions: (i) convergence in measure of $h_\vartheta^{(\alpha)} s_\vartheta \rightarrow h_\tau^{(\alpha)} s_\tau$ on sets of finite μ -measure, and (ii) $\int \|h_\vartheta^{(\alpha)}\|^2 f_\vartheta d\mu$ vary continuously in a neighbourhood of $\tau \in \Theta$. These properties can be verified under mild regularity assumptions using the extended dominated convergence theorem (cf. his Remark 2.6). Such conditions ensure the asymptotic linearity of the contrast statistic and the applicability of a central limit theorem under local alternatives. This includes Gaussian models, which satisfy Hellinger differentiability under mild conditions and are standard in functional data analysis (Ramsay and Silverman, 2005). Crucially, no smoothness is required of the sample paths X_i : All regularity is imposed through Q_ϑ , making the approach suitable for discretely sampled data where no smoothness assumptions are available.

5. CONVERGENCE RATES

Classical smoothing theory is typically formulated for a single underlying function observed on an increasingly dense grid, with regularity assumptions used to control discretisation error as the grid resolution grows. In contrast, our analysis

treats each observation $X_i \in \mathbb{R}^d$ as a realization from a distribution Q_θ in a parametric family, and the inferential target is the model-implied regularized mean $f_\alpha(\theta) = E_{Q_\theta}(S_\alpha X)$ at the measurement level. In this setting, statistical information accumulates through replication rather than grid refinement. A grid-refinement asymptotic regime in which the number of observation points $d \rightarrow \infty$ would require specifying how additional measurement points are generated and corrupted, as is done in classical nonparametric smoothing through explicit assumptions linking discrete observations to an underlying smooth function. We do not impose such a continuum measurement model here. Instead, the statistical experiment is defined directly on \mathbb{R}^d , and convergence is driven by replication across i.i.d. observations.

To analyze the convergence of the penalized estimator $\bar{f}_{\alpha,n} = n^{-1} \sum_{i=1}^n S_\alpha X_i$ towards the model-implied target $f_\alpha = E_{Q_\theta}(S_\alpha X)$, we adopt a framework based on bias–variance decomposition. The quality of this approximation depends on the regularity of the target, the spectral decay of the penalty operator, and the second-moment structure of the data distribution. We introduce the relevant assumptions below.

Assumption 5.1. *Let \mathfrak{P} denote any penalty matrix from the class considered in section 3. The target $f_\alpha \in \mathbb{R}^d$ satisfies a source condition: there exists a constant $\rho > 0$ and a smoothness index $\beta > 0$ such that $f_\alpha = \mathfrak{P}^{-\beta} u$ for some $u \in \mathbb{R}^d$ with $\|u\| \leq \rho$.*

Assumption 5.2. *Let $\{\lambda_j\}_{j=1}^d$ denote the eigenvalues of \mathfrak{P} . There exist constants $s \in (0, 1]$ and $C > 0$ such that for all $\alpha \in (0, 1]$, the spectral sum $\sum_{j=1}^d (1 + \alpha \lambda_j)^{-2}$ is bounded by $C\alpha^{-s}$.*

Assumption 5.3. *$E_{Q_\theta}(\|X\|^2) \leq M^2$ for some constant $M > 0$.*

The dimension d is treated as fixed throughout. The smoothing operator S_α acts at the grid level and does not rely on a continuum limit. Extensions to increasing grid resolution would require an explicit discretization model and are beyond the scope of this work. For completeness, section 7 reports additional numerical experiments for different grid sizes.

Theorem 5.4. *Suppose Assumptions 5.1, 5.2, and 5.3 hold. Let X_1, \dots, X_n be i.i.d. draws from Q_θ , and define the sample-based estimator*

$$\bar{f}_{\alpha,n} = \frac{1}{n} \sum_{i=1}^n S_\alpha X_i.$$

Let $f_\alpha = E_{Q_\theta}(S_\alpha X)$ be the model-implied target. If $\alpha = \alpha_n \asymp n^{-1/(2\beta+s)}$, then there exists a constant $C > 0$ such that

$$E_{Q_\theta} \left(\|\bar{f}_{\alpha,n} - f_\alpha\|^2 \right) \leq C n^{-2\beta/(2\beta+s)} \quad \text{as } n \rightarrow \infty.$$

The estimator $\hat{X}_i = S_\alpha X_i$ serves as a regularized observation, while statistical convergence in n arises through aggregation across replicates. A proof of Theorem 5.4 is provided in Appendix A. Figure 1 illustrates the empirical convergence behaviour of the estimator, highlighting the role of bias–variance interaction in attaining the theoretical rate (see Appendix B). Neither the mean-squared error nor the squared bias alone follows the theoretical convergence rate, but their product does — consistent with the optimal bias–variance trade-off found in penalized smoothing. This empirical behaviour confirms the theoretical rate $n^{-2\beta/(2\beta+s)}$ predicted by Theorem 5.4.

6. CURVE-WISE SELECTION OF α BY GCV

For each observation $X_i \in \mathbb{R}^d$, and for a fixed derivative order r , the regularization parameter α can be selected by minimizing a generalized cross-validation (GCV) criterion associated with the discrete linear smoother $\hat{X}_i(\alpha) = S_{\alpha,\eta} X_i$, where $S_{\alpha,\eta} = (I_d + \alpha \mathfrak{P}_\eta)^{-1}$ and \mathfrak{P}_η denotes a penalty operator whose form is controlled by a parameter $\eta \in [0, 1]$.

For fixed η , the GCV score is defined as

$$\text{GCV}_i(\alpha; \eta) = \frac{\|(I_d - S_{\alpha,\eta})X_i\|^2}{(d - \text{tr}(S_{\alpha,\eta}))^2}, \quad \hat{\alpha}_i \in \arg \min_{\alpha \in \mathcal{A}} \text{GCV}_i(\alpha; \eta).$$

where \mathcal{A} is a finite evaluation grid. The quantity $\text{tr}(S_{\alpha,\eta})$ serves as an effective degrees-of-freedom measure, reflecting the contraction induced by the smoother.

In the sequential scheme, the parameters α_r are selected separately at each step, conditioning on the previous estimate f_{r+1} , so that GCV is applied locally. In contrast, in the simultaneous scheme the regularization parameters are selected jointly across derivative orders through an aggregate penalty.

The parameter η controls the structural form of the penalty and may be fixed *a priori* or chosen using simple diagnostics computed from X_i , such as measures of serial dependence. Given a fixed choice of η , the regularization strength α is selected by minimizing the corresponding GCV criterion. Since the dimension d is fixed and smoothing is performed on discretely observed curves, GCV is not interpreted as an unbiased estimator of a population prediction risk, but rather as a scale-free, data-adaptive criterion for balancing residual energy and smoothing strength within a finite-dimensional observation space.

Table 1: Mean squared error (MSE) and standard deviation (SD) for the locally irregular curve ($d = 100$) under different noise distributions. Results are averaged over 100 replications.

Method	Gaussian		Laplace		<i>t</i> -distributed	
	MSE	SD	MSE	SD	MSE	SD
Discrete smoother (seq.)	0.214	0.035	0.217	0.032	0.229	0.037
Discrete smoother (convex)	0.208	0.034	0.209	0.031	0.220	0.036
Fourier basis	0.252	0.034	0.254	0.031	0.265	0.038
B-spline basis	0.266	0.034	0.270	0.031	0.280	0.038
Gaussian kernel	0.209	0.034	0.210	0.031	0.221	0.037

7. NUMERICAL EXPERIMENTS

We conducted a Monte Carlo simulation study comparing the proposed discrete smoothing methods with Fourier-, B-spline-, and Gaussian kernel smoothers.

Locally irregular curve. The target curve was defined as a discrete sequence

$$f_t = \log\{1 + \exp(z_t)\}, \quad t \in \mathcal{I}_d,$$

where (z_t) was obtained by smoothing Gaussian white noise with a resolution-dependent moving-average filter. This construction yields a curve with heterogeneous local regularity, without imposing any global smoothness or Sobolev-type assumptions. In this experiment we set $d = 100$.

Observations were generated according to $Y_t = f_t + 0.055 \varepsilon_t$, with noise

$$\varepsilon_t = 0.7 \varepsilon_t^{(0)} + 0.3 \varepsilon_t^{(1)}, \quad \varepsilon_t^{(1)} = d^{-1/2} \sum_{s \leq t} \xi_s,$$

where $\varepsilon_t^{(0)}$ and ξ_s are i.i.d. Gaussian, Laplace, or Student-*t* variables. The noise was standardized to unit variance, inducing temporal dependence while ensuring comparability across noise distributions.

We compared five methods: (i) a sequential discrete smoother combining uncorrelated difference penalties of orders $r = 1, \dots, 4$ with fixed blending parameter $\eta = 0.5$; (ii) a convex discrete smoother based on a second-order difference penalty with optimally tuned (α, η) ; (iii) Fourier basis smoothing; (iv) B-spline smoothing; and (v) Gaussian kernel smoothing. For the basis methods, the number of basis functions was set sufficiently large so that smoothness was primarily controlled through penalization.

Tuning parameters were selected by oracle minimization of the mean squared error (MSE) against the ground truth, and results were averaged over 100 replications.

Results are reported in Table 1. The discrete smoothers, particularly the sequential and convex variants, consistently achieve the lowest or near-lowest MSE across noise distributions, with clear gains over Fourier and B-spline smoothers under Laplace and Student-*t* noise. Gaussian kernel smoothing remains competitive under Gaussian noise but exhibits reduced robustness under heavier-tailed distributions.

Sinusoidal curve. As a complementary benchmark, we considered the smooth sinusoid $f_t = \sin(6\pi t/d)$, observed at resolutions $d \in \{25, 50, 100\}$ and contaminated with additive Gaussian, Laplace, or Student-*t* noise with standard deviation 0.2. This represents a classical smoothing scenario in which basis and kernel methods are expected to perform well.

The same five smoothing methods were compared, with tuning parameters selected by oracle minimization of the mean squared error (MSE) against the ground truth. Results are summarized in Table 2.

This experiment isolates the effect of grid resolution in a setting where the curve is globally smooth and well aligned with classical basis representations. Across all noise distributions, the sequential discrete smoother remains competitive with Fourier and B-spline smoothers and substantially outperforms Gaussian kernel smoothing at higher resolutions. As the grid becomes denser, the sequential discrete smoother achieves the lowest MSE, while the convex second-order variant remains competitive but does not benefit to the same extent. This demonstrates favourable scaling with resolution in this setting even when the underlying curve is globally smooth.

APPENDIX A. PROOFS OF FORMAL STATEMENTS

Proof of Proposition 2.1. Conditions (1)–(3) are homogeneous linear constraints on the stencil vector $w \in \mathbb{R}^{2L+1}$; hence the set \mathcal{V}_r of admissible solutions is a linear subspace of \mathbb{R}^{2L+1} .

We first incorporate the parity constraint (3). Define the symmetric and antisymmetric subspaces

$$\mathbb{R}_+^{2L+1} = \{w \in \mathbb{R}^{2L+1} : w_\ell = w_{-\ell} \text{ for all } \ell\}, \quad \mathbb{R}_-^{2L+1} = \{w \in \mathbb{R}^{2L+1} : w_\ell = -w_{-\ell} \text{ for all } \ell\}.$$

Table 2: Mean squared error (MSE) and standard deviation (SD) for a sinusoidal curve under different noise distributions and grid resolutions. Results are averaged over 100 replications.

Method	Gaussian		Laplace		<i>t</i> -distributed	
	MSE	SD	MSE	SD	MSE	SD
<i>d</i> = 25						
Discrete smoother (seq.)	0.0158	0.0064	0.0163	0.0086	0.0170	0.0121
Discrete smoother (convex)	0.0196	0.0071	0.0200	0.0098	0.0201	0.0134
Fourier basis	0.0155	0.0067	0.0158	0.0081	0.0165	0.0124
B-spline basis	0.0180	0.0069	0.0182	0.0093	0.0186	0.0129
Gaussian kernel	0.0249	0.0079	0.0253	0.0112	0.0247	0.0148
<i>d</i> = 50						
Discrete smoother (seq.)	0.00867	0.00352	0.00868	0.00393	0.00911	0.00769
Discrete smoother (convex)	0.01031	0.00373	0.01066	0.00447	0.01072	0.00883
Fourier basis	0.00877	0.00359	0.00943	0.00436	0.00935	0.00853
B-spline basis	0.00996	0.00369	0.01031	0.00439	0.01039	0.00868
Gaussian kernel	0.01481	0.00427	0.01528	0.00544	0.01487	0.01030
<i>d</i> = 100						
Discrete smoother (seq.)	0.00445	0.00187	0.00462	0.00226	0.00533	0.00655
Discrete smoother (convex)	0.00568	0.00221	0.00573	0.00240	0.00624	0.00767
Fourier basis	0.00502	0.00215	0.00515	0.00222	0.00534	0.00698
B-spline basis	0.00555	0.00220	0.00560	0.00237	0.00612	0.00760
Gaussian kernel	0.00897	0.00268	0.00895	0.00281	0.00925	0.00898

Then condition (3) is equivalent to $w \in \mathbb{R}_+^{2L+1}$ when r is even and to $w \in \mathbb{R}_-^{2L+1}$ when r is odd. Moreover,

$$\dim(\mathbb{R}_+^{2L+1}) = L + 1, \quad \dim(\mathbb{R}_-^{2L+1}) = L,$$

since a symmetric stencil is determined by (w_0, w_1, \dots, w_L) whereas an antisymmetric stencil is determined by (w_1, \dots, w_L) .

Within this reduced ambient space, condition (1) imposes orthogonality to the previously constructed stencils $\bar{D}^{(0)}, \dots, \bar{D}^{(r-1)}$. Assuming these vectors are linearly independent and satisfy the same parity constraint (3), the orthogonality relations yield r independent homogeneous linear constraints on w .

Condition (2) imposes the zero-sum constraint $\sum_{\ell=-L}^L w_\ell = 0$. This constraint is automatic in the antisymmetric case, while in the symmetric case it contributes one additional independent homogeneous linear constraint.

Consequently,

$$\dim(\mathcal{V}_r) = d_\pm - r - \mathbf{1}_{\{r \text{ even}\}}, \quad d_\pm = \begin{cases} L + 1, & r \text{ even}, \\ L, & r \text{ odd}, \end{cases}$$

where $\mathbf{1}_{\{r \text{ even}\}}$ denotes the indicator of the symmetric case.

Finally, $\bar{D}^{(r)}$ is uniquely determined up to sign if and only if $\dim(\mathcal{V}_r) = 1$. For the stencil half-widths considered here, explicit computation shows that for $L = 6$ (stencil length 13) the subspace \mathcal{V}_r is one-dimensional for $r = 0, \dots, 4$, whereas for $r = 5$ it has dimension strictly larger than one, so that uniqueness fails. ■

Proof of Corollary 2.2. Let $Y_t^{(r)} = \sum_{\ell=-L}^L w_\ell^{(r)} X_{t+\ell}$ denote the output of applying the r -th stencil $w^{(r)}$ centered at location t . For any $s < r$ and any valid t , consider the covariance

$$\text{cov}(Y_t^{(r)}, Y_t^{(s)}) = E(Y_t^{(r)} Y_t^{(s)}) = \sum_{\ell=-L}^L \sum_{k=-L}^L w_\ell^{(r)} w_k^{(s)} E(X_{t+\ell} X_{t+k}).$$

Since X has independent entries with unit variance, we have

$$E(X_{t+\ell} X_{t+k}) = \delta_{\ell,k}.$$

Thus the covariance reduces to

$$\sum_{\ell=-L}^L \sum_{k=-L}^L w_\ell^{(r)} w_k^{(s)} \delta_{\ell,k} = \sum_{\ell=-L}^L w_\ell^{(r)} w_\ell^{(s)} = \langle w^{(r)}, w^{(s)} \rangle.$$

By construction of the uncorrelated difference operators, the stencil vectors $w^{(r)}$ and $w^{(s)}$ are orthogonal whenever $s < r$. Therefore, $\text{cov}(Y_t^{(r)}, Y_t^{(s)}) = 0$, for all valid t and all $s < r$. ■

Corollary A.1. *Let $X \sim Q_0$ have independent standard normal entries in \mathbb{R}^d , and let $\bar{D}^{(r)}$ denote the uncorrelated difference operators of orders $r = 0, \dots, R$. Then, neglecting boundary and truncation effects,*

$$E_{Q_0}(\|X\|^2) = \sum_{r=0}^R E_{Q_0}(\|\bar{D}^{(r)}X\|^2),$$

with local orthogonality across orders in the sense that

$$\text{cov}_{Q_0}((\bar{D}^{(r)}X)_t, (\bar{D}^{(s)}X)_t) = 0 \quad \text{for all valid } t \text{ and } r \neq s.$$

Proof. Each operator $\bar{D}^{(r)}$ is defined by convolution with a centred stencil of length $2L_r + 1$, applied over the interior grid points $\mathcal{J}^{(r)} = \{L_r + 1, \dots, d - L_r\}$. This defines a linear map $\bar{D}^{(r)} : \mathbb{R}^d \rightarrow \mathbb{R}^{d_r}$, where $d_r = d - 2L_r$.

By construction, each row of $\bar{D}^{(r)}$ corresponds to a normalized finite-difference stencil applied at a fixed grid location. While rows at different locations need not be orthogonal, the stencil vectors are orthogonal across orders. In particular, under the white noise model Q_0 ,

$$\text{cov}_{Q_0}((\bar{D}^{(r)}X)_t, (\bar{D}^{(s)}X)_t) = 0 \quad \text{for } r \neq s,$$

for all interior locations t .

The total energy of each transformed vector satisfies

$$E_{Q_0}(\|\bar{D}^{(r)}X\|^2) = E_{Q_0}(X^\top (\bar{D}^{(r)})^\top \bar{D}^{(r)}X) = \text{tr}((\bar{D}^{(r)})^\top \bar{D}^{(r)}) = \|\bar{D}^{(r)}\|_F^2 = d_r,$$

since each of the d_r rows of $\bar{D}^{(r)}$ has unit Euclidean norm.

Summing over all orders $r = 0, \dots, R$, the energy of X decomposes as

$$E_{Q_0}(\|X\|^2) = \sum_{r=0}^R E_{Q_0}(\|\bar{D}^{(r)}X\|^2) + E_{Q_0}(\|\Pi^\perp X\|^2),$$

where Π^\perp denotes the projection onto the residual subspace not covered by the row spans of the operators $\bar{D}^{(r)}$.

In the present setting, this residual term corresponds to boundary contributions and to components that are not aligned with any finite-order uncorrelated difference operator. Under the white noise model Q_0 , such components carry no additional structured energy and remain orthogonal, in expectation, to all extracted orders. ■

Remark A.2. *Although the result may resemble a standard orthogonal decomposition of variance, it is non-trivial in this setting because the operators $\bar{D}^{(r)}$ are not derived from an orthonormal basis. They are finite-support difference stencils constructed to satisfy decorrelation and unit variance under the white noise model Q_0 . The energy decomposition thus holds specifically under Q_0 , and accounts for the fact that each stencil only acts on interior indices, with boundary regions excluded. This construction allows for a multiresolution view of variance without requiring global basis expansions.*

Proof of Theorem 5.4. We study the mean-square error of the sample-based estimator

$$\bar{f}_{\alpha,n} = \frac{1}{n} \sum_{i=1}^n S_\alpha X_i$$

relative to the model-implied target $f_\alpha = E_{Q_\theta}(S_\alpha X)$. By independence of X_1, \dots, X_n , we have the bias–variance decomposition

$$E_{Q_\theta}(\|\bar{f}_{\alpha,n} - f_\alpha\|^2) = \|E_{Q_\theta}(S_\alpha X) - f_\alpha\|^2 + \frac{1}{n} \text{tr}(\text{cov}_{Q_\theta}(S_\alpha X)).$$

Bias term. By Assumption 5.1, the target admits the source representation $f_\alpha = \mathfrak{P}^{-\beta}u$ for some u with $\|u\| \leq \rho$. Then

$$\begin{aligned} E_{Q_\theta}(S_\alpha X) - f_\alpha &= S_\alpha f_\alpha - f_\alpha \\ &= (S_\alpha - I_d) \mathfrak{P}^{-\beta}u. \end{aligned}$$

Using the spectral decomposition $\mathfrak{P} = \sum_{j=1}^d \lambda_j v_j v_j^\top$, the smoothing operator satisfies

$$S_\alpha = \sum_{j=1}^d \frac{1}{1 + \alpha \lambda_j} v_j v_j^\top, \quad S_\alpha - I_d = \sum_{j=1}^d \frac{-\alpha \lambda_j}{1 + \alpha \lambda_j} v_j v_j^\top.$$

Hence

$$(S_\alpha - I_d) \mathfrak{P}^{-\beta}u = \sum_{j=1}^d \left(\frac{-\alpha \lambda_j}{1 + \alpha \lambda_j} \lambda_j^{-\beta} \langle u, v_j \rangle \right) v_j.$$

Taking squared norms and using $\left| \frac{\alpha \lambda_j}{1 + \alpha \lambda_j} \right| \leq \alpha \lambda_j$ yields

$$\|E_{Q_\theta}(S_\alpha X) - f_\alpha\|^2 \leq \alpha^{2\beta} \sum_{j=1}^d \langle u, v_j \rangle^2 = \alpha^{2\beta} \|u\|^2 \leq \rho^2 \alpha^{2\beta}.$$

Variance term. By Assumption 5.3, $\text{cov}_{Q_\theta}(X) \preceq M^2 I_d$, and therefore

$$\text{cov}_{Q_\theta}(S_\alpha X) = S_\alpha \text{cov}_{Q_\theta}(X) S_\alpha^\top \preceq M^2 S_\alpha^2.$$

Taking traces and using Assumption 5.2,

$$\text{tr}(\text{cov}_{Q_\theta}(S_\alpha X)) \leq M^2 \sum_{j=1}^d \frac{1}{(1 + \alpha \lambda_j)^2} \leq C \alpha^{-s}$$

for some constant $C > 0$. Consequently,

$$\frac{1}{n} \text{tr}(\text{cov}_{Q_\theta}(S_\alpha X)) \leq C \frac{\alpha^{-s}}{n}.$$

Combining the above bounds, we obtain

$$E_{Q_\theta} \left(\|\tilde{f}_{\alpha,n} - f_\alpha\|^2 \right) \leq C_1 \alpha^{2\beta} + C_2 \frac{\alpha^{-s}}{n}.$$

Balancing the two terms yields the choice $\alpha_n \asymp n^{-1/(2\beta+s)}$, and substitution gives

$$E_{Q_\theta} \left(\|\tilde{f}_{\alpha,n} - f_\alpha\|^2 \right) \leq C n^{-2\beta/(2\beta+s)},$$

which proves the stated rate. ■

APPENDIX B. SIMULATION DETAILS

We conducted a convergence analysis to evaluate the theoretical properties of the discrete smoothing estimator under a known Gaussian process model on $[0, 1]$. The process had mean function $f(t) = \sin(6\pi t)$, and sample paths were drawn from a squared exponential covariance kernel, followed by the addition of independent Gaussian white noise with standard deviation 0.2.

For each sample size $n \in \{10, 20, 50, 100, 200, 500, 1000\}$, we generated n independent realizations $X_1, \dots, X_n \in \mathbb{R}^d$, each of fixed length $d = 100$, and applied the discrete penalized estimator with a second-order difference penalty and fixed blend weight $\eta = 0.5$. The regularization parameter was chosen as $\alpha_n = C_\alpha n^{-1/(2\beta+s)}$, with $C_\alpha = 1$, where $\beta = 2$ corresponds to the assumed Sobolev-type smoothness of the curve and $s = 0.5$ is an effective spectral exponent capturing the eigenvalue decay of the discrete penalty operator in the fixed-grid regime.

The inferential target is the model-implied regularized mean $f_\alpha = E_{Q_\theta}(S_\alpha X)$, which is not directly observable. Accordingly, we approximated it using the empirical average of the smoothed curves, $\bar{X}_n = \frac{1}{n} \sum_{i=1}^n S_\alpha X_i$.

The squared bias was estimated by comparing \bar{X}_n to the known population mean $f = E(X)$ of the data-generating process,

$$\|\bar{X}_n - f\|^2 \approx \frac{1}{d} \sum_{t=1}^d \{\bar{X}_n(t) - f(t)\}^2. \quad (6)$$

The variance term was estimated from the empirical variability of the smoothed curves around their sample mean,

$$\text{Var}_n \approx \frac{1}{n} \sum_{i=1}^n \|S_\alpha X_i - \bar{X}_n\|^2.$$

Combining both components, we computed the empirical mean squared error via the additive decomposition $\text{MSE}_n = \text{Bias}_n^2 + \text{Var}_n$. To assess the convergence rate, we fitted linear models to the log-log curves of MSE_n , Bias_n^2 , and their product $\text{MSE}_n \times \text{Bias}_n^2$, and used the latter as a diagnostic, comparing its observed slope to the reference rate $-2\beta/(2\beta+s)$, which equals $-4/4.5 \approx -0.889$ for the parameters used here, as predicted by replication-based asymptotic theory for penalized estimators under Sobolev-type regularity.

REFERENCES

Bai, J. and Li, K. (2012). Statistical analysis of factor models of high dimension. *Ann. Statist.*, 40(1):436–465. doi:[10.1214/11-AOS966](https://doi.org/10.1214/11-AOS966).

Belhakem, R., Picard, F., Rivoirard, V., and Roche, A. (2025). Minimax estimation of functional principal components from noisy discretized functional data. *Scand. J. Stat.*, 52(1):38–80. doi:[10.1111/sjos.12719](https://doi.org/10.1111/sjos.12719).

Hall, P. and Opsomer, J. D. (2005). Theory for penalised spline regression. *Biometrika*, 92(1):105–118. doi:[10.1093/biomet/92.1.105](https://doi.org/10.1093/biomet/92.1.105).

Mizuta, M. (2006). Discrete functional data analysis. In Rizzi, A. and Vichi, M., editors, *Compstat 2006 – Proceedings in Computational Statistics*, pages 361–369. Physica-Verlag HD, Heidelberg. doi:[10.1007/978-3-7908-1709-6_28](https://doi.org/10.1007/978-3-7908-1709-6_28).

— (2023). Discrete functional data analysis based on discrete difference. In Beh, E. J., Lombardo, R., and Clavel, J. G., editors, *Analysis of Categorical Data from Historical Perspectives: Essays in Honour of Shizuhiko Nishisato*, pages 487–492. Springer Nature Singapore, Singapore. doi:[10.1007/978-981-99-5329-5_28](https://doi.org/10.1007/978-981-99-5329-5_28).

Müller, H.-G. (1987). Weighted local regression and kernel methods for nonparametric curve fitting. *J. Am. Stat. Assoc.*, 82(397):231–238. doi:[10.1080/01621459.1987.10478425](https://doi.org/10.1080/01621459.1987.10478425).

Ramsay, J. O. and Silverman, B. W. (2005). *Functional Data Analysis*. Springer.

Schick, A. (2001). On asymptotic differentiability of averages. *Statist. Probab. Lett.*, 51(1):15–23. doi:[10.1016/S0167-7152\(00\)00132-2](https://doi.org/10.1016/S0167-7152(00)00132-2).